Selective inhibition of Cx43 hemichannels by Gap19 and its impact on myocardial ischemia/reperfusion injury

Journal: Basic Research in Cardiology

Nan Wang[1#], Elke De Vuyst[1#], Raf Ponsaerts[2#], Kerstin Boengler[3], Nicolás Palacios-Prado[4], Joris Wauman[5], Charles P. Lai[6], Marijke De Bock[1], Elke Decrock[1], Melissa Bol[1], Mathieu Vinken[7], Vera Rogiers[7], Jan Tavernier[5], W. Howard Evans[8], Christian C. Naus[9], Feliksas F. Bukauskas[4], Karin R. Sipido[10], Gerd Heusch[11], Rainer Schulz[3], Geert Bultynck[2$], and Luc Leybaert[1$]

[1]Department of Basic Medical Sciences - Physiology group, Faculty of Medicine and Health Sciences, Ghent University, Ghent, Belgium
[2]Laboratory of Molecular and Cellular Signaling - Department of Cellular and Molecular Medicine, Campus Gasthuisberg O/N-1 bus 802, KU Leuven, Leuven, Belgium
[3]Physiologisches Institut, Justus-Liebig Universität Giessen, Giessen, Germany
[4]Dominick P. Purpura Department of Neuroscience Department of Neuroscience, Albert Einstein College of Medicine, Bronx, NY, USA
[5]VIB Department of Medical Protein Research - Cytokine Receptor Laboratory, Faculty of Medicine and Health Sciences, Ghent University, Ghent, Belgium
[6]Departments of Neurology and Radiology, Massachusetts General Hospital, and Neuroscience Program, Harvard Medical School, Charlestown, MA, USA
[7]Department of Toxicology, Faculty of Medicine and Pharmacy, Vrije Universiteit Brussel, Brussels, Belgium
[8]Department of Medical Biochemistry and Immunology, Cardiff University School of Medicine, Cardiff, United Kingdom
[9]Department of Cellular and Physiological Sciences, Life Sciences Institute, Faculty of Medicine, University of British Columbia, Vancouver, BC, Canada
[10] Division of Experimental Cardiology, Department of Cardiovascular Diseases, Katholieke Universiteit Leuven, Belgium
[11]Institute for Pathophysiology, Universitätsklinikum Essen, Essen, Germany

Address correspondence to:

Luc Leybaert (M.D., Ph.D.)
E-mail: Luc.Leybaert@UGent.be

[#]These authors contributed equally

[$]These authors share senior authorship

Supplementary Material

Online Fig. S1

A

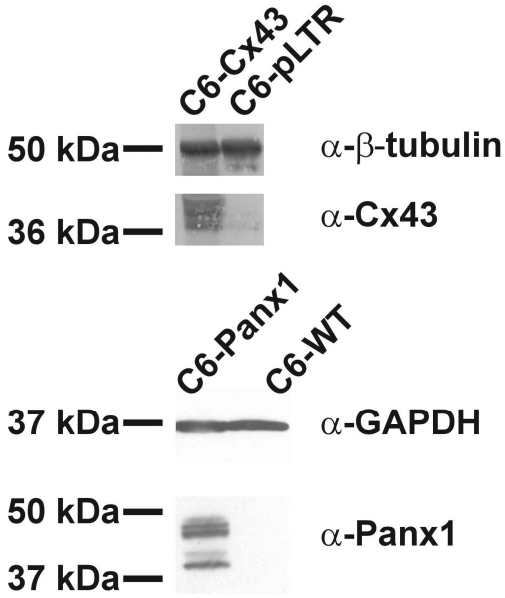

B

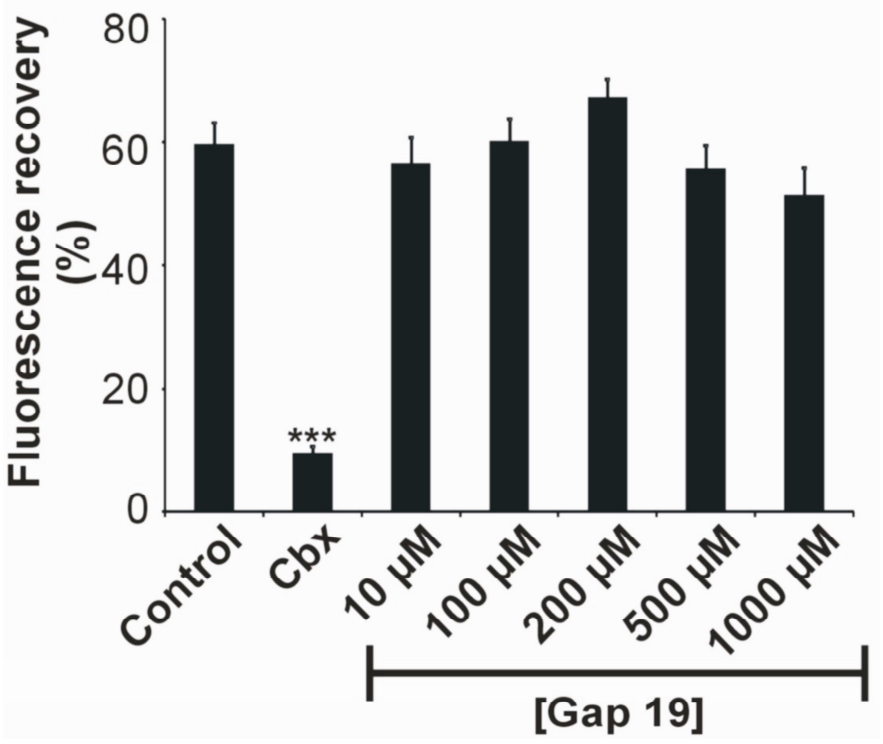

Online Fig. S2

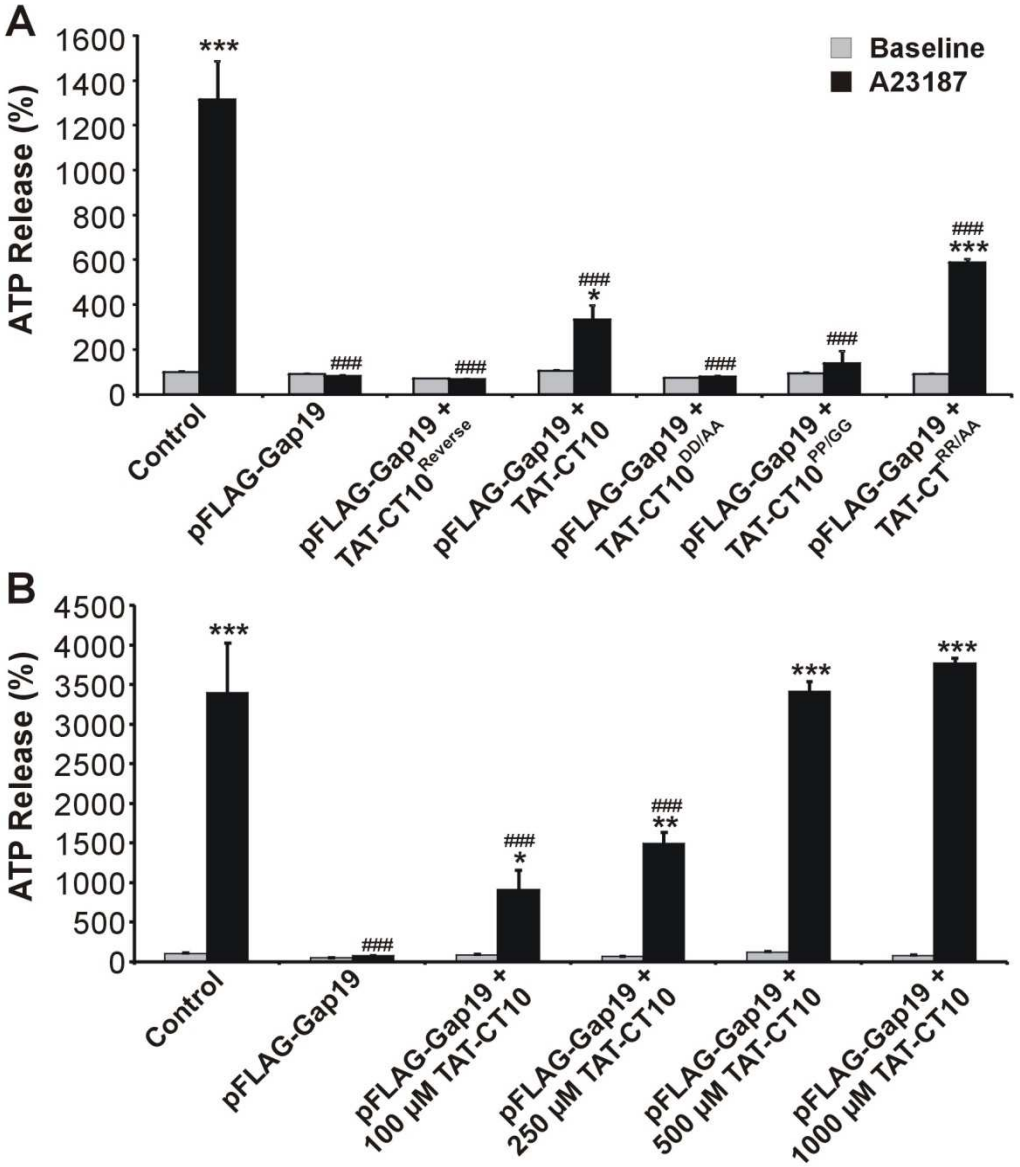

Online Fig. S3

A

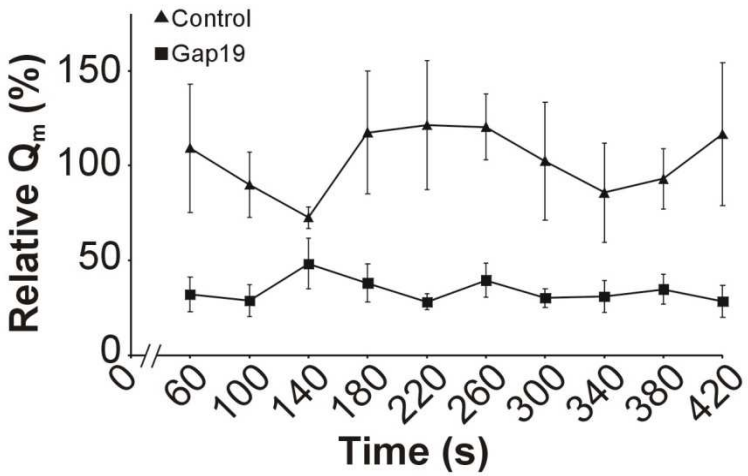

B

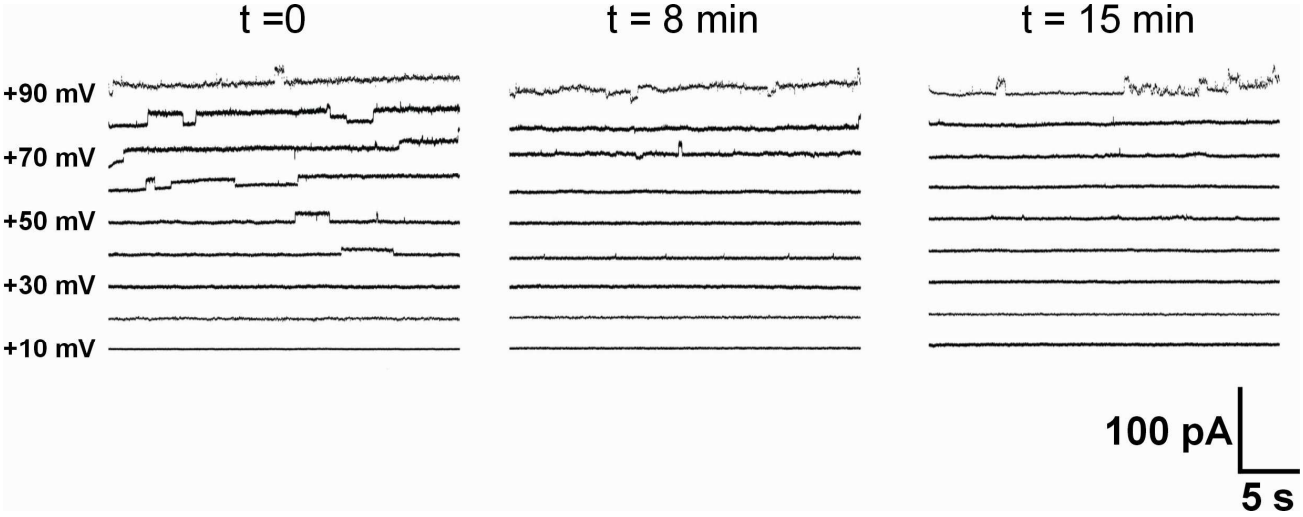

Online
Fig. S4

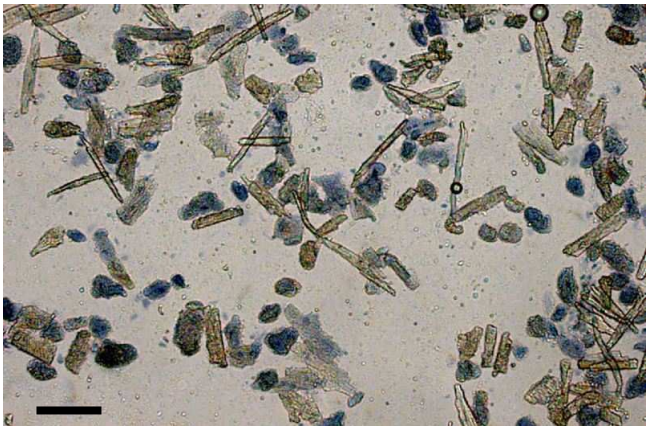

Online
Fig. S5

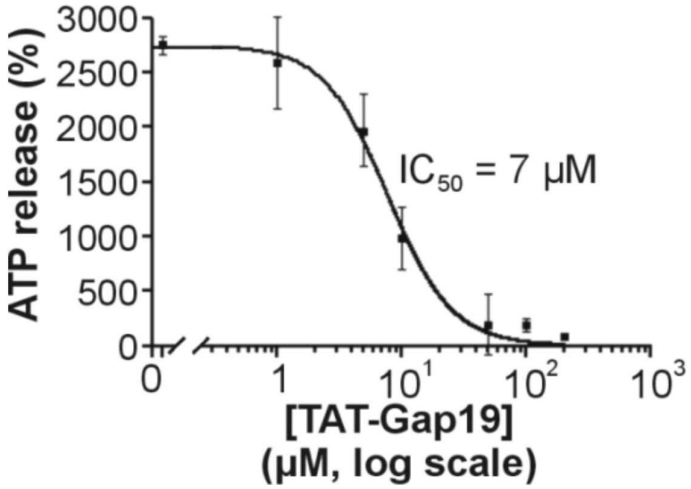

Online Fig. S6

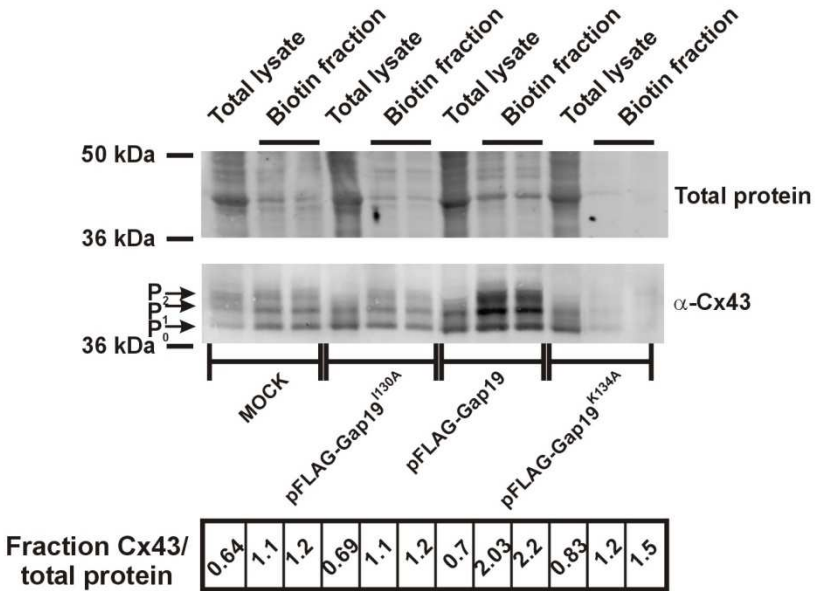

LEGENDS

Online Fig S1. A. Western blotting demonstrating Cx43 and Panx1 expression in the C6 cell lines used. β-tubulin was the loading control for Cx43 and GADPH for Panx1. **B. Gap19 does not inhibit dye coupling in C6-Cx43 cells.** Exposing C6-Cx43 cells to different concentrations of Gap19 (10-1000 µM) during 1 h had no effect on dye coupling measured with FRAP. The GJ blocker carbenoxolone (Cbx, 25 µM, 1 h) was used as a positive control (n = 5). *** indicates significantly different from control with $p < 0.001$.

Online Fig. S2. The effect of pFLAG-Gap19 is reversed by the CT10 peptide. A. Transiently transfecting C6-Cx43 cells with pFLAG-Gap19 completely abolished $[Ca^{2+}]_i$-triggered ATP release. CT10 peptide (100 µM, 30 min) partially reversed the pFLAG-Gap19 inhibitory effect, while $CT10^{reverse}$ had no effect. The two aspartate and the two proline residues are crucial for the CT10 effect (n = 12). **B.** The partial reversal of pFLAG-Gap19 inhibitory effects by TAT-CT10 becomes complete with higher concentrations of TAT-CT10 (n = 12). The fact that higher concentrations were necessary to obtain complete reversal (compared to Fig. 2F) indicates that the plasmid expression system generates higher Gap19 concentrations in the cell as compared to extracellulary added Gap19. Star signs indicate significantly different from baseline, number signs indicate significantly different from control.

Online Fig. S3. Unitary current activities as a function of time. A. Data from C6-Cx43 cells. Graph depicting Q_m as a function of time in voltage-clamp experiments. Q_m was normalized to the average value recorded in control. After formation of a gigaseal, the membrane was disrupted giving access to the cell (time zero). Depolarizing voltage steps to +70 mV (30 s) were repeatedly applied over a total recording period of 360 s and the corresponding Q_m was quantified. The effect of Gap19 (400 µM, present in the pipette) was apparent from the start of the recording (1 min after rupturing the plasma membrane in whole-cell recording) and the Q_m trace remained stable over the entire recording period, demonstrating ~75 % inhibition of the control Q_m trace. Taken together, this suggests that Gap19 acts within 1 min. The lower variability of the currents with Gap19 is related to inhibition of unitary event activity that lies at the basis of the noise observed in the control recording (n = 6 for control and 8 for Gap19). **B.** Data from acutely isolated pig ventricular myocytes. Example traces recorded at different points in time with Gap19 (100 µM) in the

recording pipette. Isolated cardiomyocytes were stepped to positive V_m ranging from +10 mV to +90 mV (30 s) in 10 mV increments. Time 0 indicates onset of recording just after patch break. Effect of Gap19 on voltage-dependence of hemichannel openings was progressively enhanced over time and reached steady-state within 8 min.

Online Fig. S4. Example image illustrating a typical trypan blue cell viability staining. After exposure to *in vitro* ischemia/reperfusion, rounded cardiomyocytes were stained by trypan blue while rod-shaped healthy cells were trypan blue negative. Bar = 100 µm.

Online Fig. S5. Concentration-dependent inhibition of hemichannel activities by TAT-conjugated Gap19. Inhibition of $[Ca^{2+}]_i$-triggered ATP release by TAT-Gap19 was characterized by an IC_{50} of ~7 µM (Hill coefficient = 2). ATP release in ordinate expresses baseline-subtracted measurements; data obtained in C6-Cx43 cell cultures (n = 5). Compare to Fig . 1D.

Online Fig. S6. pFLAG-Gap19 increases the hemichannel fraction. Transient transfection of C6-Cx43 cells with pFLAG-Gap19 increased the hemichannel fraction (Biotin fraction) present at the plasma membrane, while the inactive mutants pFLAG-Gap19^{I130A} and pFLAG-Gap^{K134A} had no effect (data shown representative of 3 different experiments). The Biotin fraction showed clearly increased phosphorylation, especially at the P1 band.

TABLES

Table S1. Overview of the different peptides used in this study.

Peptide	Sequence
Gap19	^{128}KQIEIKKFK^{136}
Gap19^{I130A}	KQAEIKKFK
Gap19^{E131A}	KQIAIKKFK
Gap19$^{I130A/E131A}$	KQAAIKKFK
FLAG-Gap19	DYKDDDDK-GGSGGS-^{128}KQIEIKKFK^{136}
TAT-Gap19	YGRKKRRQRRR-^{128}KQIEIKKFK^{136}
TAT-CT10	YGRKKRRQRRR-^{373}SRPRPDDLEI^{382}
TAT-CT10^{reverse}	YGRKKRRQRRR-IELDDPRPRS
TAT-CT10$^{DD/AA}$	YGRKKRRQRRR-SRPRPAALEI
TAT-CT10$^{PP/GG}$	YGRKKRRQRRR-SRGRGDDLEI
TAT-CT10$^{RR/AA}$	YGRKKRRQRRR-SAPAPDDLEI
^{10}Panx1	^{74}WRQAAFVDSY^{83}
Scr^{10}Panx1	FSVYWAQADR

Table S2. DNA sequences cloned in the pcDNA5/FRT-EGFP vector.

Mutation	Forward primer	Reverse primer
Q129A	5’-GGCTCGGGCGGCTCCAAGGCGATCGAGATA-3’	5’-CTTGAACTTCTTTATCTCGATCGCCTTGGA-3’
I130A	5’-AAGGCGGCTCGGGCGGATCCAAGCAGGCAGAGATA-3’	5’-TCTCTGCCTGCTTGGATCCGCCCGAGCCGCCTTTG-3’
K134A	5’-CCAAGCAGATAGAGATAAAGGCCTTCAAGT-3’	5’-GACTCGAGTTACTTGAAGGCCTTTATCTCT-3’
I130A/K134A	5’-GGCTCCAAGCAGGCAGAGATAAAGGCCTTCAAGTA-3’	5’-AGTTACTTGAAGGCCTTTATCTCTGCCTGCTTGGA

SUPPLEMENTAL MATERIALS AND METHODS

An expanded methods section

Synthetic peptides,

Synthetic peptides used in this study were all obtained from Lifetein (Edison, New Jersey, USA). The identity of the peptides was confirmed by mass spectrometry and purity was ≥ 90 %.

Gap19 coding plasmids

The DNA sequence encoding Gap 19, separated from an N-terminal FLAG-tag by a double Gly-Gly-Ser linker, was cloned in a dual expression vector, pcDNA5/FRT-eGFP, which was modified with a second expression cassette allowing integration (*BamH*I-*Xho*I) of annealed oligos encoding FLAG-2x(GGS)-Gap19 under control of a second CMV promoter; 5'-GATCCACCATGGACTACAAAGACGACGACGACAAAGGCGGCTCGGGCGGCTCCA AGCAGATAGAGATAAAGAAGTTCAAGTAAC-3' and 5'-TCGAGTTACTTGAACTTC TTTATCTCTATCTGCTTGGAGCCGCCCGAGCCGCCTTTGTCGTCGTCGTCTTTGTA GTCCATGGTG-3'. Several mutated versions of this pFLAG-Gap 19 construct were generated using the Quikchange Site-directed mutagenesis kit ® (Stratagene, La Jolla, California, USA). The primer sequences used to generate the mutations are shown in Online Resource Table S2. All primers contained extra restriction sites to check the quality of the mutagenesis (Q129A: *Pvu*I; I130A: *BamH*I; K134A: *Stu*I and I130A/K134A: *Stu*I). All constructs were verified by DNA sequence analysis. Transfection with the Transfectin® reagent (Biorad) was done 6 h after seeding the cells at a density of 50000 cells/cm^2. The transfection efficiency was about 70 %. ATP release measurements were performed 24 h after transfection and SLDT 48 h after transfection.

Uptake studies of labeled Gap19 peptide

Peptide uptake studies were performed on C6 glioma cells stably transfected with Cx43 (C6-Cx43) [11]. The cells were incubated with 200 µM fluorescein isothiocyanate (FITC) coupled Gap19, FITC-coupled Gap19I130A or fluorescein alone for 30 min at 37 °C. Subsequently, cells were washed extensively with PBSD to remove excessive fluorescence and fixed with

4 % paraformaldehyde (in PBSD; 20 min at room temperature). After fixation the cells were exposed to phalloidin coupled to Alexa 546 (0.165 µM, 20 min at room temperature; Invitrogen, Merelbeke, Belgium) to label F-actin. After washing, the cells were mounted with Vectashield (Vector Laboratories, Labconsult, Brussels, Belgium) and imaged with a confocal microscope (LSM510, Carl Zeiss, Zaventem, Belgium) equipped with a x63 objective using 488 nm (fluorescein) or 543 nm (phalloidin) excitation lasers. Z-stacks were taken every 100 nm and the average intensity projection (the projection of the 3D Z-stacks on a 2D image) was calculated with ImageJ software (ImageJ 1.44; NIH, Bethesda, Maryland, USA; http://rsb.info.nih.gov/ij). In this image, the regions of interest (ROI) were defined in the cytoplasm of each cell, based on the phalloidin staining, making use of ImageJ software. All cell ROI had the same surface area.

ATP release experiments

ATP release experiments were performed on C6-Cx43 cells [11], C6-Panx1 cells [5] and HeLa cells [10]. C6-Cx43 and C6-Panx1 cells were maintained in DMEM:Ham's F12 (1:1 - Invitrogen, Merelbeke, Belgium) and HeLa-Cx40 cells were grown in DMEM, all supplemented with 10% fetal bovine serum, 2 mM glutamine, 10 U/ml penicillin, 10 µg/ml streptomycin and 0.25 µg/ml fungizone. Cells were seeded at a density of 50000 cells/cm² and used for experiments the next day (non-confluent low density cultures).
ATP release was measured directly in the medium above the cells using luciferin-luciferase and luminometric measurements with a plate reader protocol as previously described in [3]. Baseline measurements were carried out on separate cultures with HBSS-HEPES (Hanks' balanced salt solution - pH 7.4) vehicle only. All applied agents were added to the medium of the cell cultures in the CO_2 incubator at 37 °C, for the times indicated in the text, and were not present during stimulation and measurement to avoid interference with luminometry.

Junctional conductance measurements

Experiments were performed on a Novikoff rat hepatoma cell line that endogenously expresses wild-type Cx43. These cells were grown in Swim's S-77 medium supplemented with 4 mM glutamine, 20 % horse serum and 5 % fetal bovine serum. Junctional conductance was measured in cell pairs (cell-1 and -2) using dual whole-cell patch-clamp. Each cell was voltage clamped with separate amplifiers (EPC-8, HEKA Instruments, Bellmore, NY, USA)

and data were digitized and acquired with a BNC-2090 A/D converter (National Instruments, Austin, TX, USA). Analysis was performed with custom-developed software (Trexler Technologies). Cells were grown onto glass coverslips and placed on an experimental chamber mounted on the stage of an Olympus IX70 inverted microscope (Olympus America, Center Valley, PA, USA). Cells were continuously perfused (at room temperature) with modified Krebs-Ringer solution that contained (in mM): NaCl, 140; KCl, 4; $CaCl_2$, 2; $MgCl_2$, 1; glucose, 5; pyruvate, 2; Hepes, 5 (pH 7.4). Pipette solution, with or without 400 μM of Gap19, contained (in mM): KCl, 140; NaAsp, 10; K_2ATP, 3; $MgCl_2$, 1; $CaCl_2$, 0.2; EGTA, 2; Hepes, 5 (pH 7.2). Transjunctional voltage (V_j) was applied by varying the voltage in cell-1 with repeated ramps of ±10 mV in amplitude and 600 ms in duration, and keeping the voltage constant in cell-2. Junctional current (I_j) was measured as the change in current in cell-2 (ΔI_2), and because I_j has the same orientation as V_j a negative sign is used, thus $I_j = -\Delta I_2$. Junctional conductance (G_j) was calculated as $G_j = I_j/V_j$. Octanol (5 mM) was perfused at the end of every experiment to completely block G_j and rule out the presence of cytoplasmic bridges.

Gap junction dye transfer

GJ dye transfer was investigated with FRAP (fluorescent recovery after photobleaching) and SLDT (scrape loading and dye transfer) methods. For FRAP, confluent C6-Cx43 cultures grown on plastic Petri dishes (Becton Dickinson, Erembodegem, Belgium) were loaded with 5-carboxyfluorescein diacetate acetoxy methylester (CFDA-AM, 20 μM) in HBSS-HEPES for 1 h at room temperature, followed by 30 min de-esterification. Fluorescence within a single cell was photobleached by spot exposure to the 488 nm line of an Argon laser (10 s). Fluorescence imaging (at 488 nm excitation) was performed using a custom-made video-rate confocal laser scanning microscope with a x40 water immersion objective (CFI Plan Fluor, NA 1.4, Nikon Benelux, Brussels, Belgium) and fluorescence recovery was measured over a 5 min time period after photobleaching.

For SLDT, confluent monolayer cultures were washed with nominally Ca^{2+}-free HBSS-HEPES and then incubated for 1 min in this solution containing 0.4 mM 6-carboxy fluorescein (6-CF). A linear scratch was made across the culture using a syringe needle and the cells were left for another minute in the same solution. Cultures were then washed 4 times with HBSS-HEPES, left for 15 min at room temperature and images were taken with a Nikon TE300 inverted microscope with FITC excitation/emission settings, a x10 objective and a Nikon DS-5M camera (Analis, Namur, Belgium). A fluorescence diffusion profile was

extracted from the images, fitted to a mono-exponential decaying function and a spatial constant of intercellular dye spread was determined.

Unitary current hemichannel measurements

Hela-Cx43 cells were placed in a recording chamber containing a bath solution composed of (in mM) 150 NaCl, 4 KCl, 2 $MgCl_2$, 5 glucose, 5 HEPES, 2 pyruvate, 2 $CaCl_2$, 2 CsCl, 1 $BaCl_2$ (pH = 7.4). Recording pipettes contained (in mM): 130 KCl, 10 Na-aspartate, 0.26 $CaCl_2$, 5 HEPES, 2 EGTA, 5 TEACl, 1 $MgCl_2$ (pH = 7.2). The free Ca^{2+} concentration of the pipette solution was estimated to be ~50 nM as calculated with WEBMAX (http://www.stanford.edu/~cpatton/webmaxcS.htm)

For the experiments on pig cardiomyocytes, left ventricular cardiomyocytes from adult domestic pigs were enzymatically isolated [9]. Briefly, the left anterior descending coronary artery was cannulated, and the cells were dissociated by enzymatic tissue digestion throughout Langendorff perfusion at 37°C. During the recording, isolated cells were initially perfused with the standard Tyrode solution (in mM): 137 NaCl, 5.4 KCl, 1.8 $CaCl_2$, 0.5 $MgCl_2$, 10 glucose, 11.8 HEPES and pH adjusted to 7.4. When recording unitary hemichannel currents, the solution was switched to one with the same composition but with all K^+ replaced by Cs^+ and additional 1 mM Ba^{2+}. During the 30s depolaeization steps, the time dependent currents such as Na^+ and Ca^{2+} did not contaminate the observation of connexin hemichannel opening. The standard pipette solution was composed of (in mM): 120 CsCl, 5 NaCl, 10 TEACl, 1 $CaCl_2$, 1 $MgCl_2$, 2 MgATP, 10 EGTA, 10 HEPES and pH adjusted to 7.2. The free Ca^{2+} concentration of the pipette solution was estimated to be ~50 nM as calculated with WEBMAX. During metabolic inhibition, myocytes were dialyzed by pipette solution with slight modifications: 120 CsCl, 3 NaCl, 10 TEACl, 1 $CaCl_2$, 2 $MgCl_2$, 2 MgATP, 1 NaH_2PO_4, 5 sodium pyruvate, 1 NaADP, 10 HEPES, 10 EGTA, pH 7.2. Pyruvate, P_i, Mg and ADP that are metabolic substrates for oxidative phosphorylation in control were included to allow ATP depletion during metabolic inhibition.

Single channel recordings in Hela cells and cardiomyocytes were performed as previously described [2], making use of an EPC 7 PLUS patch-clamp amplifier (HEKA Elektronik, Germany) and Axon Axopatch 200B (Axon Instruments/Molecular Devices, USA) respectively. Data were acquired at 4 kHz using a NI USB-6221 data acquisition device from National Instruments (Austin, TX) and Clampex 10.2 acquisition software (Axon instruments/Moleuclar Devices, USA). All currents in whole-cell configuration were filtered

at 1 kHz (7-pole Besselfilter). Membrane potentials were corrected for the liquid junction potentials.

Surface plasmon resonance (SPR)

SPR experiments were performed using a Biacore 2000 system. Equal amounts of > 95 % pure biotinylated peptides (biotin-gap19, biotin-L2 and biotin-L2-reverse) were immobilized on flow cells of a streptavidin-coated sensor chip (BR-1000-32, Biacore AB, Uppsala Sweden) using HEPES buffer (in mM: 10 HEPES, 1 EDTA, 100 NaCl) with 0.005 % P-20 at pH 7.4. Measurements with analyte were done at a flow rate of 30 µl/min in HEPES running buffer at pH 6.8. Binding of analyte was verified at different concentrations, in random order (injection volume 120 µl). The chip-surface was regenerated by injection of 10 µl of alkalic buffer (50 mM NaOH, 1 M NaCl) at 10 µl/min. The CT tail of Cx43 was used as analyte and measured in analytically prepared buffers. Background signals obtained from the reference flow cell, containing immobilized L2-reverse peptide, were subtracted to generate response curves. For quantification of resonance signal of repeated measurements, the resonance unit value recoded at 1 second before the stop of injection was taken for each sensorgram (acquisition at 1 Hz), corresponding to the last resonance unit value in the association phase of the sensorgram.

Purification of the CT tail of Cx43

The complete CT tail of Cx43 was recombinantly expressed in BL21(DE3) and purified as GST-fusion protein. Briefly, the pGEX6p2-Cx43CT cDNA (AA 255-382) plasmid construct, obtained from P. Sorgen [4], was transformed into BL21(DE3) bacteria. Protein expression was induced by 0.1 mM IPTG at 28 °C for 4 h in diluted overnight-grown bacterial cultures when the OD600 reached 0.6 to 0.8. Bacterial cells were lysed using sonication and the soluble fraction was collected by centrifugation for further purification on glutathione Sepharose 4B. GST was removed from the immobilized GST-Cx43CT protein by using 40 U PreScission protease for 4 h (GE Healthcare, Buckinghamshire, United Kingdom) and the soluble fraction containing the purified CT tail was collected, dialysed against PBS using Slide-A-Lyzer (cutoff: 3 kDa) and stored at -80 °C awaiting further analysis. Protein concentration was determined using the BCA method. Protein purity and cleavage efficiency was analyzed using SDS-PAGE, followed by total protein staining using Gelcode Blue™

stain reagent (Thermo Scientific). All samples contained at least 10 µM of the complete CT tail protein with a purity of > 90 %.

In vivo cardiac ischemia/reperfusion

Eight to 10 week old C57/Bl6 mice were subjected to 30 min ischemia by LAD coronary artery ligation followed by release of the ligature and 120 min reperfusion [1,8]. The area at risk was measured by Evans Blue intracardially injected after ischemia/reperfusion and the size of the ischemic zone was determined by 2,3,3-triphenyl tetrazolium chloride (TTC) staining. Gap19 or Gap19^{I130A} were injected in the jugular vein 10 min prior to ischemia dissolved in 0.9 % NaCl solution. All procedures were approved by the Bioethical Committee of the district of Düsseldorf, Germany, and conformed to the Guide for the Care and Use of Laboratory Animals (NIH publication No. 85-23, revised 1996).

Western blotting

Cell lysates were extracted by treatment of confluent cultures with RIPA buffer (25 mM Tris, 50 mM NaCl, 0.5 % NP-40, 0.5 % deoxycholate, 0.1 % SDS, 5.5 % β-glycerophosphate, 1 mM dithiothreitol, 2 % phosphatase inhibitor cocktail, and 2 % mini EDTA-free protease inhibitor cocktail) and sonicated by three 10 s pulses. Protein concentration was determined with a Biorad DC protein assay kit, and absorbance was measured with a 590 nm long-pass filter. Proteins were separated by electrophoresis on a 10 % SDS-poly-acrylamide gel and transferred to a nitrocellulose membrane (GE Healthcare). Blots were probed with a rabbit polyclonal anti-rat Cx43 antibody (1/10000; Sigma) or a rabbit polyclonal anti-rat Panx1 [6] (1/1000) followed by alkaline phosphatase conjugated goat anti-rabbit IgG (1/8000, Sigma) and detection was done with nitro blue tetrazolium/5-bromo-4-chloro-3-indolyl phosphate reagent (Zymed, Invitrogen). Multiple bands on the Panx1 blots are probably the consequence of different glycosylated forms [7].

Isolation of the Cx43 hemichannel fraction

The Cx43 hemichannel fraction was isolated from a confluent monolayer of C6-Cx43 cells with the Pierce cell surface protein isolation kit (Thermo Scientific, Erembodegem, Belgium) according to the manufacturer's instructions. Briefly, a monolayer of C6-Cx43 cells was

exposed to PBS containing 0.25 mg/ml sulfo-NHS-SS-biotin for 2h at 4 °C. The biotinylation reaction was stopped by adding quenching solution and incubated for 5 min at room temperature. Subsequently, the cells were scraped and lysed with the provided lysis buffer, mixed with Neutravidine^{TM} agarose and incubated overnight at 4 °C with end-over-end mixing. The biotinylated proteins were eluted from the Neutravidine^{TM} agarose through heating of the mixture in SDS-PAGE sample buffer. Separation of the biotinylated proteins was done on a 10 % SDS-PAGE, followed by Western blotting and detection of Cx43.

REFERENCES

1. Boengler K, Buechert A, Heinen Y, Roeskes C, Hilfiker-Kleiner D, Heusch G, Schulz R (2008) Cardioprotection by ischemic postconditioning is lost in aged and STAT3-deficient mice. Circ Res 102: 131-135 doi:10.1161/CIRCRESAHA.107.164699

2. Contreras JE, Saez JC, Bukauskas FF, Bennett MV (2003) Gating and regulation of connexin 43 (Cx43) hemichannels. Proc Natl Acad Sci U S A 100: 11388-11393 doi:10.1073/pnas.1434298100

3. De Vuyst E, Decrock E, Cabooter L, Dubyak GR, Naus CC, Evans WH, Leybaert L (2006) Intracellular calcium changes trigger connexin 32 hemichannel opening. EMBO J 25: 34-44 doi:10.1038/sj.emboj.7600908

4. Hirst-Jensen BJ, Sahoo P, Kieken F, Delmar M, Sorgen PL (2007) Characterization of the pH-dependent interaction between the gap junction protein connexin43 carboxyl terminus and cytoplasmic loop domains. J Biol Chem 282: 5801-5813 doi:10.1074/jbc.M605233200

5. Lai CP, Bechberger JF, Thompson RJ, MacVicar BA, Bruzzone R, Naus CC (2007) Tumor-suppressive effects of pannexin 1 in C6 glioma cells. Cancer Res 67: 1545-1554 doi:10.1158/0008-5472.CAN-06-1396

6. Penuela S, Bhalla R, Gong XQ, Cowan KN, Celetti SJ, Cowan BJ, Bai D, Shao Q, Laird DW (2007) Pannexin 1 and pannexin 3 are glycoproteins that exhibit many distinct characteristics from the connexin family of gap junction proteins. J Cell Sci 120: 3772-3783 doi:10.1242/jcs.009514

7. Penuela S, Bhalla R, Nag K, Laird DW (2009) Glycosylation regulates pannexin intermixing and cellular localization. Mol Biol Cell 20: 4313-4323 doi:10.1091/mbc.E09-01-0067

8. Schwanke U, Konietzka I, Duschin A, Li X, Schulz R, Heusch G (2002) No ischemic preconditioning in heterozygous connexin43-deficient mice. Am J Physiol Heart Circ Physiol 283: H1740-H1742 doi:10.1152/ajpheart.00442.2002

9. Stankovicova T, Szilard M, De Scheerder I, Sipido KR (2000) M cells and transmural heterogeneity of action potential configuration in myocytes from the left ventricular wall of the pig heart. Cardiovasc Res 45: 952-960

10. Traub O, Eckert R, Lichtenberg-Frate H, Elfgang C, Bastide B, Scheidtmann KH, Hulser DF, Willecke K (1994) Immunochemical and electrophysiological characterization of murine connexin40 and -43 in mouse tissues and transfected human cells. Eur J Cell Biol 64: 101-112.

11. Zhu D, Caveney S, Kidder GM, Naus CC (1991) Transfection of C6 glioma cells with connexin 43 cDNA: analysis of expression, intercellular coupling, and cell proliferation. Proc Natl Acad Sci U S A 88: 1883-1887.